Biochem. J. (2010) **430**, 393–404 (Printed in Great Britain) doi:10.1042/BJ20100483

14-3-3 binding to LRRK2 is disrupted by multiple Parkinson's disease-associated mutations and regulates cytoplasmic localization

R. Jeremy NICHOLS*[1,3], Nicolas DZAMKO*, Nicholas A. MORRICE*[2], David G. CAMPBELL*, Maria DEAK*, Alban ORDUREAU*, Thomas MACARTNEY*, Youren TONG†, Jie SHEN†, Alan R. PRESCOTT‡ and Dario R. ALESSI*[3]

*MRC Protein Phosphorylation Unit, College of Life Sciences, University of Dundee, Dow Street, Dundee DD1 5EH, Scotland, U.K., †Center for Neurologic Diseases, Brigham and Women's Hospital, Program in Neuroscience, Harvard Medical School, Boston, MA 02115, U.S.A., and ‡Division of Cell Biology and Immunology, College of Life Sciences, University of Dundee, Dow Street, Dundee DD1 5EH, Scotland, U.K.

LRRK2 (leucine-rich repeat protein kinase 2) is mutated in a significant number of Parkinson's disease patients, but still little is understood about how it is regulated or functions. In the present study we have demonstrated that 14-3-3 protein isoforms interact with LRRK2. Consistent with this, endogenous LRRK2 isolated from Swiss 3T3 cells or various mouse tissues is associated with endogenous 14-3-3 isoforms. We have established that 14-3-3 binding is mediated by phosphorylation of LRRK2 at two conserved residues (Ser^{910} and Ser^{935}) located before the leucine-rich repeat domain. Our results suggests that mutation of Ser^{910} and/or Ser^{935} to disrupt 14-3-3 binding does not affect intrinsic protein kinase activity, but induces LRRK2 to accumulate within discrete cytoplasmic pools, perhaps resembling inclusion bodies. To investigate links between 14-3-3 binding and Parkinson's disease, we studied how 41 reported mutations of LRRK2 affected 14-3-3 binding and cellular localization. Strikingly, we found that five of the six most common pathogenic mutations (R1441C, R1441G, R1441H, Y1699C and I2020T) display markedly reduced phosphorylation of Ser^{910}/Ser^{935} thereby disrupting interaction with 14-3-3. We have also demonstrated that Ser^{910}/Ser^{935} phosphorylation and 14-3-3 binding to endogenous LRRK2 is significantly reduced in tissues of homozygous LRRK2(R1441C) knock-in mice. Consistent with 14-3-3 regulating localization, all of the common pathogenic mutations displaying reduced 14-3-3-binding accumulated within inclusion bodies. We also found that three of the 41 LRRK2 mutations analysed displayed elevated protein kinase activity (R1728H, ~2-fold; G2019S, ~3-fold; and T2031S, ~4-fold). These results provide the first evidence suggesting that 14-3-3 regulates LRRK2 and that disruption of the interaction of LRRK2 with 14-3-3 may be linked to Parkinson's disease.

Key words: cytoplasmic localization, 14-3-3 protein, leucine-rich repeat protein kinase 2 (LRRK2), Parkinson's disease, pathogenic mutation, phosphorylation.

INTRODUCTION

Autosomal dominant missense mutations within the gene encoding for the LRRK2 (leucine-rich repeat protein kinase 2) predispose humans to develop PD (Parkinson's disease) [1,2]. LRRK2 is a large enzyme (2527 residues), consisting of leucine-rich repeats (residues 1010–1287), a GTPase domain (residues 1335–1504), a COR [C-terminal of ROC (Ras of complex GTPase domain)] domain (residues 1517–1843), a serine/threonine protein kinase domain (residues 1875–2132) and a WD40 repeat (residues 2231–2276) [3]. Patients with LRRK2 mutations generally develop PD with clinical symptoms indistinguishable from idiopathic PD at approx. 60–70 years of age [4]. Mutations in LRRK2 account for 4 % of familial PD, and are observed in 1 % of sporadic PD patients [4]. Over 40 missense mutations have been reported that are scattered throughout LRRK2 [5,6].

The activity, as well as localization, of a subset of mutant forms of LRRK2 has been analysed in previous work using various forms of recombinant LRRK2 expressed and assayed using diverse approaches [3,7]. This has revealed that the most frequent mutation, comprising an amino acid substitution of the highly conserved Gly^{2019} located within the subdomain VII-DFG motif of the kinase domain, enhances protein kinase activity approx. 2-fold [8–10], suggesting that LRRK2 inhibitors might be useful for the treatment of PD. It was also reported that various mutants such as LRRK2(R1441C) and LRRK2(Y1699C) accumulated within discrete cytosolic pools, resembling inclusion bodies that were suggested to consist of aggregates of misfolded protein [9].

In the present study we have demonstrated that endogenous LRRK2 interacts with endogenous 14-3-3 protein isoforms and that this binding is mediated via phosphorylation of LRRK2 at Ser^{910} and Ser^{935}. We provide evidence that disruption of 14-3-3-binding induces LRRK2 to accumulate within cytoplasmic pools, similar in appearance to those reported previously for the LRRK2(R1441C) and LRRK2(Y1699C) mutants [9]. Comparing the properties of 41 PD-associated mutant forms of LRRK2 strikingly revealed that ten of these displayed markedly reduced phosphorylation of Ser^{910}/Ser^{935} and 14-3-3 binding that included five common well-characterized pathogenic mutations (R1441C, R1441G, R1441H, Y1699C and I2020T). We also observed that most mutants displaying reduced Ser^{910}/Ser^{935} phosphorylation and association with 14-3-3 accumulated within cytoplasmic pools. These results provide the first evidence

Abbreviations used: CDC, cell division cycle; DIG, digoxigenin; DMEM, Dulbecco's modified Eagle's medium; DTT, dithiothreitol; FBS, fetal bovine serum; GFP, green fluorescent protein; HEK-293, human embryonic kidney; Hsp90, heat-shock protein 90; IPI, International Protein Index; KLH, keyhole-limpet haemocyanin; LRRK2, leucine-rich repeat protein kinase 2; MARK3, microtubule affinity-regulating kinase 3; PD, Parkinson's disease; ROC, Ras of complex GTPase domain; COR, C-terminal of ROC; SILAC, stable isotope labelling of amino acids; TBST, Tris-buffered saline with Tween 20.

[1] Present address: Parkinson's Institute, 675 Almanor Ave., Sunnyvale, CA 94085, U.S.A.
[2] Present address: The Beatson Institute for Cancer Research, Garscube Estate, Switchback Road, Bearsden, Glasgow G61 1BD, Scotland, U.K.
[3] Correspondence may be addressed to either of these authors (jnichols@parkinsonsinstitute.org or d.r.alessi@dundee.ac.uk).

that a significant number of PD-associated mutations inhibit Ser^{910}/Ser^{935} phosphorylation, disrupting 14-3-3 binding and leading to accumulation of LRRK2 within cytoplasmic pools. Our present study will stimulate further work to explore whether disruption of 14-3-3 binding to LRRK2 is linked to the development of PD.

EXPERIMENTAL

Reagents and general methods

Tissue-culture reagents were from Life Technologies. P81 phosphocellulose paper was from Whatman and [γ-^{32}P]ATP was from PerkinElmer. All peptides were synthesized by Pepceuticals. The Flp-in T-REx system was from Invitrogen, and stable cell lines, generated according to the manufacturer's instructions by selection with hygromycin, have been described previously [11]. Restriction enzyme digests, DNA ligations and other recombinant DNA procedures were performed using standard protocols. All mutagenesis was carried out using the QuikChange® site-directed mutagenesis kit (Stratagene). DNA constructs used for transfection were purified from *Escherichia coli* DH5α cells using Qiagen or Invitrogen plasmid Maxi kits according to the manufacturer's instructions. All DNA constructs were verified by DNA sequencing, which was performed by the Sequencing Service, School of Life Sciences, University of Dundee, Dundee, Scotland, U.K., using DYEnamic ET terminator chemistry (Amersham Biosciences) with automated DNA sequencers (Applied Biosystems).

Buffers

Lysis buffer contained 50 mM Tris/HCl, pH 7.5, 1 mM EGTA, 1 mM EDTA, 1 % (w/v) (1 mM) sodium orthovanadate, 10 mM sodium β-glycerophosphate, 50 mM NaF, 5 mM sodium pyrophosphate, 0.27 M sucrose, 1 mM benzamidine and 2 mM PMSF and was supplemented with 1 % Triton X-100. Buffer A contained 50 mM Tris/HCl, pH 7.5, 50 mM NaCl, 0.1 mM EGTA and 0.27 M sucrose. λ phosphatase reactions were carried out in buffer A supplemented with 1 mM $MnCl_2$, 2 mM DTT (dithiothreitol) and 0.5 μg of λ phosphatase.

Antibodies

Anti-LRRK2-(100–500) (S348C and S406C) and anti-LRRK2-(2498–2514) (S374C) antibodies have been described previously [8]. The antibody against LRRK2 phospho-Ser^{910} (S357C) was generated by injection of the KLH (keyhole-limpet haemocyanin)-conjugated phospho-peptide VKKKSNpSISVGEFY (where pS is phospho-serine) into sheep and was affinity-purified by positive and negative selection against the phospho- and de-phospho-peptides respectively. Antibody against LRRK2 phospho-Ser^{935} (S814C) was generated by injection of the KLH-conjugated phospho-peptide NLQRHSNpSLGPIFDH into sheep and was affinity-purified by positive and negative selection against the phospho- and de-phospho-peptides respectively. Anti-GFP (green fluorescent protein) antibody (S268B) was raised against the recombinant GFP and affinity-purified against the antigen. Anti-FLAG M2 antibody and the affinity matrix were from Sigma (A2220). The Nanotrap GFP-binder affinity matrix was from ChromoTek. Rabbit polyclonal antibody recognizing 14-3-3 (K-19, SC-629) and control rabbit IgG (SC-2027) antibody were from Santa Cruz Biotechnology. Anti-Hsp90 (heat-shock protein 90) antibody was from Cell Signaling Technology (#4877). Anti-MARK3 (microtubule affinity-regulating kinase 3) was from Upstate Biotechnology (#05-680).

Cell culture, treatments and cell lysis

HEK-293 (human embryonic kidney) and Swiss 3T3 cells were cultured in DMEM (Dulbecco's modified Eagle's medium) supplemented with 10 % FBS (fetal bovine serum), 2 mM glutamine and 1× antimycotic/antibiotic solution (1 × penicillin/streptomycin/amphotericin B; Invitrogen). HEK-293 T-REx cell lines were cultured in DMEM supplemented with 10 % FBS and 2 mM glutamine, 1× antimycotic/antibiotic solution, 15 μg/ml blastocidin and 100 μg/ml hygromycin. Cell transfections were performed by the polyethyleneimine method [12]. T-REx cultures were induced to express the indicated protein by inclusion of 1 μg/ml doxycycline in the culture medium for 24 h. Per 15 cm dish, cells washed once with PBS and lysed *in situ* with 1.0 ml of lysis buffer, on ice, then centrifuged at 16000 ***g*** at 4 °C for 10 min. Protein concentrations were determined using the Bradford method with BSA as the standard.

SILAC (stable isotope labelling of amino acids) medium

SILAC DMEM (high glucose without $NaHCO_3$, L-glutamine, arginine, lysine and methionine; Biosera #A0347) was prepared with 10 % dialysed FBS (Hyclone) and supplemented with methionine, glutamine, $NaHCO_3$ and labelled or unlabelled arginine and lysine. Cells harbouring GFP-tagged proteins were cultured in SILAC DMEM for three passages at a 1:10 ratio with the following isotopic labelling. For GFP compared with wild-type LRRK2, L-arginine (84 μg/ml; Sigma–Aldrich) and L-lysine (146 μg/ml; Sigma–Aldrich) were added to the GFP 'light' medium, whereas ^{13}C-labelled L-arginine and ^{13}C-labelled L-lysine (Cambridge Isotope Laboratory) were added to the GFP–LRRK2 wild-type 'heavy' medium at the same concentrations. For the GFP compared with LRRK2(G2019S) experiments, L-arginine and L-lysine were added to the GFP 'light' medium and ^{13}C/^{15}N-labelled L-arginine and ^{13}C/^{15}N-labelled L-lysine (Cambridge Isotope Laboratory) to the GFP–LRRK2(G2019S) 'heavy' medium. The amino acid concentrations are based on the formula for normal DMEM (Invitrogen). Once prepared, the SILAC medium was mixed well and filtered through a 0.22-μm filter (Millipore). Metabolically labelled cells were induced to express GFP or the GFP–LRRK2 fusion protein for 24 h by inclusion of doxycycline in the culture medium.

SILAC labelling and MS

Cells metabolically labelled and induced to express GFP, wild-type LRRK2 or LRRK2(G2019S) were lysed in lysis buffer supplemented with 1 % Triton X-100 at 0.5 ml per 10 cm dish. For each condition individually, 9 mg of cell lysate was subjected to individual immunoprecipitation with a 20 μl of bed volume of GFP-binder agarose beads for 1 h at 4 °C. Beads were washed once with 5 ml and then with 10 ml of lysis buffer supplemented with 1 % Triton-X 100 and 300 mM NaCl. Beads were then washed once with 5 ml and then once with 10 ml of storage buffer. Bead-associated proteins were eluted with 1× NuPAGE LDS sample buffer (Invitrogen) for 10 min at 70 °C then passed through a 0.22 μm Spin-X column (Corning). Control GFP eluates were combined with either eluates of wild-type LRRK2 or LRRK2(G2019S) in equal amounts and reduced and alkylated as above. Samples were resolved on a 12 % Novex gel for only one half of the gel. Gels were stained with Colloidal Blue

overnight and destained for 3 h. The entire lane was excised in nine bands in total and digested with trypsin as described previously [13]. The digests were separated on a Biosphere C_{18} trap column [0.1 mm (internal diameter)×2 mm; Nanoseparations] connected to a PepMap C_{18} nano column (75 μm×15 cm; Dionex Corporation) fitted to a Proxeon Easy-LC nanoflow LC-system (Proxeon Biosystems) with solvent A (2 % acetonitrile/0.1 % formic acid/98 % water) and solvent B (90 % acetonitrile/10 % water/0.09 % formic acid). Samples (10 μl; a total of 2 μg of protein) were loaded with a constant flow of 7 μl/min on to the trap column in solvent A and washed for 3 min at the same flow rate. After trap enrichment, peptides were eluted with a linear gradient of 5–50 % solvent B over 90 min with a constant flow of 300 nl/min. The HPLC system was coupled to a linear ion-trap–orbitrap hybrid mass spectrometer (LTQ-Orbitrap XL, Thermo Fisher Scientific) via a nanoelectrospray ion source (Proxeon Biosystems) fitted with a 5 cm Picotip FS360-20-10 emitter. The spray voltage was set to 1.2 kV and the temperature of the heated capillary was set to 200 °C. Full-scan MS survey spectra (*m*/*z* 350–1800) in profile mode were acquired with the LTQ-Orbitrap with a resolution of 60 000 after accumulation of 500 000 ions. The five most intense peptide ions from the preview scan in the LTQ-Orbitrap were fragmented by collision-induced dissociation (normalized collision energy 35 %, activation Q 0.250 and activation time 30 ms) in the LTQ-Orbitrap after the accumulation of 10 000 ions. Maximal filling times were 1000 ms for the full scans and 150 ms for the MS/MS scans. Precursor ion-charge state screening was enabled and all unassigned charge states, as well as singly charged species, were rejected. The lock mass option was enabled for survey scans to improve mass accuracy. Data were acquired using the Xcalibur software.

LC-MS data analysis using MaxQuant

The raw mass spectrometric data files obtained for each experiment were collated into a single quantified dataset using MaxQuant (version 1.0.13.13; http://www.maxquant.org) and the Mascot search engine (Matrix Science, version 2.2.2) software. Enzyme specificity was set to that of trypsin. Other parameters used within the software: variable modifications, methionine oxidation; database, target-decoy human MaxQuant (ipi.HUMAN.v3.52.decoy) (containing 148 380 database entries); labels, R6K4 (for GFP compared with wild-type LRRK2) or R10K8 [for GFP compared with LRRK2(G2019S)]; MS/MS tolerance, 0.5 Da; top MS/MS peaks per 100 Da, 5; maximum missed cleavages, 2; maximum of labelled amino acids, 3; FDR (false discovery rate), 1 %.

Phosphorylation site identification by MS

Endogenous and recombinant LRRK2 was immunoprecipitated from 50 mg of Swiss 3T3 lysate or T-REx cells induced to express FLAG–LRRK2 cell lysate using anti-LRRK2-(100–500)– or anti-FLAG–agarose respectively. Immunoprecipitates were eluted from the affinity matrices using 2× LDS sample buffer or 200 μg/ml FLAG peptide then filtered through a 0.2 μm Spin-X column before reduction with 10 mM DTT and alkylation with 50 mM iodoacetamide. Samples were heated for 10 min at 70 °C and resolved on 4–12 % Novex gels before staining with Colloidal Blue (Invitrogen). Bands corresponding to LRRK2 were excised and digested with trypsin as described previously [13]. Samples were analysed on an LTQ-Orbitrap XL mass spectrometer as described above, except that the top five ions were fragmented in the linear ion-trap using multistage activation of the neutral loss of phosphoric acid from the parent ion (neutral loss masses=49, 32.33 and 24.5 for $z=2$, 3 and 4 respectively). Mascot generic files were created from the raw files using raw2msm (a gift from Professor Matthias Mann, Max Planck Institute of Biochemistry, Martinsried, Germany) and were searched on a local Mascot server (http://www.matrixscience.com) using the IPI (International Protein Index) mouse database for endogenous LRRK2 or the IPI human database for recombinant LRRK2.

Immunological procedures

Cell lysates (10–30 μg) were resolved by electrophoresis on SDS/polyacrylamide gels or Novex 4–12 % gradient gels, and electroblotted on to nitrocellulose membranes. Membranes were blocked with 5 % (w/v) skimmed milk in TBST [Tris-buffered saline with Tween 20: 50 mM Tris/HCl, pH 7.5, 0.15 M NaCl and 0.1 % (v/v) Tween 20]. For phospho-specific antibodies, primary antibody was used at a concentration of 1 μg/ml, diluted in 5 % skimmed milk in TBST with the inclusion of 10 μg/ml dephosphorylated peptide. All other antibodies were used at 1 μg/ml in 5 % (w/v) milk in TBST. Detection of immuno-complexes was performed using either fluorophore-conjugated secondary antibodies (Molecular Probes) followed by visualization using an Odyssey infrared imaging system (LI-COR Biosciences) or by horseradish-peroxidase-conjugated secondary antibodies (Pierce) and an enhanced chemiluminescence reagent. For immunoprecipitations, antibody was non-covalently coupled to Protein G–Sepharose at a ratio of 1 μg of antibody/μl of beads, or anti-FLAG M2–agarose was utilized. Cell lysates were incubated with coupled antibody for 1 h. To assess Ser^{935} phosphorylation, total LRRK2 levels and 14-3-3 binding in mouse tissues, LRRK2 was immunoprecipitated from 6 mg of whole-tissue lysate using 15 μg of antibody coupled to 15 μl of Protein G–Sepharose. Ser^{910} phosphorylation was assessed following immunoprecipitation from 10 mg of tissue lysate. Immuno-complexes were washed twice with lysis buffer supplemented with 0.3 M NaCl and twice with buffer A. Precipitates were re-suspended in LDS sample buffer and subjected to immunoblot analysis. DIG (digoxigenin)-labelled 14-3-3 for use in overlay far-Western blot analysis was prepared as described in [14]. To directly assess 14-3-3 interaction with LRRK2, immunoprecipitates were electroblotted on to nitrocellulose membranes and blocked with 5 % skimmed milk for 30 min. After washing with TBST, membranes were incubated with DIG-labelled 14-3-3 diluted to 1 μg/ml in 5 % BSA in TBST overnight at 4 °C. DIG-labelled 14-3-3 was detected with horseradish-peroxidase-labelled anti-DIG Fab fragments (Roche).

LRRK2 immunoprecipitation kinase assays

Transfected cell lysates (500 μg) were subjected to immuno-precipitation with a 5 μl bed volume of anti-FLAG–agarose for 1 h. Beads were washed twice with lysis buffer supplemented with 300 mM NaCl, and twice with buffer A. Peptide kinase assays were set up in a total volume of 50 μl with immunoprecipitated LRRK2 in 50 mM Tris/HCl, pH 7.5, 0.1 mM EGTA, 10 mM $MgCl_2$ and 0.1 mM [γ-^{32}P]ATP (~300–500 c.p.m./pmol) in the presence of 200 μM long variant of the LRRKtide peptide substrate (RLGRDKYKTLRQIRQGNTKQR) [10,11] or the Nictide peptide substrate (RLGWWRFYTLRRARQGNTKQR) [11]. Reactions were terminated by applying 30 μl of the reaction mixture on to P81 phosphocellulose paper and immersing in 50 mM phosphoric acid. After extensive washing, the radioactivity in the reaction products were quantified by Cerenkov counting. One half of the remaining reaction was subjected to immunoblot analysis using the Odyssey infrared imaging system

A

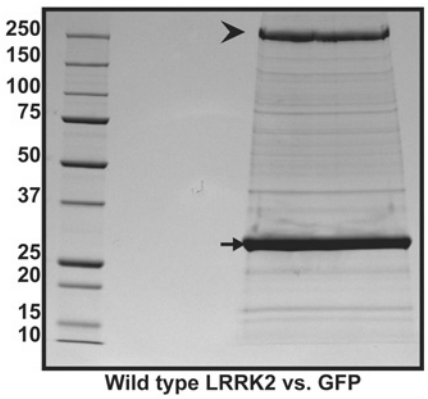

wild type LRRK2 vs. GFP Protein Name	Uniprot	Peptides analyzed (#)	Sequence Coverage [%]	Mol. Weight [kDa]	PEP	Ratio H/L
Leucine-rich repeat kinase 2	Q5S007	81	29.7	286.1	0	47.5
14-3-3 zeta/delta	P63104	4	5.7	27.7	6.00E-18	30.8
14-3-3 theta	P27348	7	15.5	27.8	1.05E-31	30.7
14-3-3 epsilon	P62258	6	14.5	29.2	1.57E-39	20.4
14-3-3 beta/alpha	P31946	5	5.7	28.1	7.75E-14	20.4
14-3-3 eta	Q04917	5	5.7	28.2	7.75E-14	20.4
Cdc37 (Hsp90 co-chaperone)	Q16543	2	5.3	44.5	2.67E-22	15.5
Hsp 90-alpha	P07900	29	16.3	98.2	7.23E-161	6.0
Hsp 90-beta	P08238	27	17	83.3	1.73E-134	5.6

B

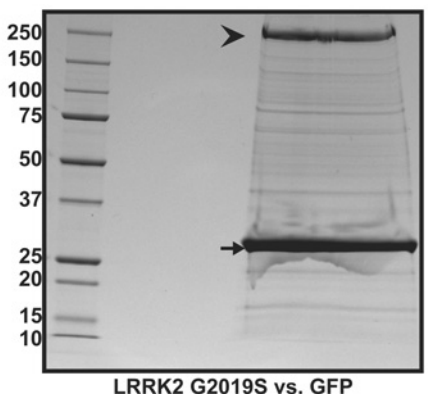

LRRK2 [G2019S] vs. GFP Protein Name	Uniprot	Peptides analyzed	Sequence Coverage [%]	Mol. Weight [kDa]	PEP	Ratio H/L
Leucine-rich repeat kinase 2	Q5S007	86	29.7	286.1	0	47.5
14-3-3 theta	P27348	6	15.5	27.8	3.58E-42	13.2
14-3-3 beta/alpha	P31946	4	5.7	28.1	1.98E-15	13.2
14-3-3 zeta/delta	P63104	4	5.7	27.7	7.27E-22	12.8
14-3-3 gamma	P61981	4	4	28.3	3.89E-14	12.0
14-3-3 epsilon	P62258	6	14.1	29.2	1.48E-28	10.9
Cdc37 (Hsp90 co-chaperone)	Q16543	6	18.5	44.5	1.09E-30	8.1
Hsp 90-alpha	P07900	32	19.3	98.2	3.77E-245	5.1
Hsp 90-beta	P08238	32	20.9	83.3	1.47E-200	4.9

Figure 1 Quantitative MS identifies 14-3-3 as an LRRK2 interactor

HEK-293 cells stably expressing GFP, wild-type full-length GFP–LRRK2 or full-length GFP–LRRK2(G2019S) mutant were cultured for multiple passages in either R6K4 SILAC medium (GFP–LRRK2) or R10K8 SILAC medium [GFP–LRRK2(G2019S)] or normal R0K0 SILAC medium (GFP). Cells were lysed and equal amounts of lysates from GFP and GFP–LRRK2 (**A**) or GFP and GFP–LRRK2(G2019S) (**B**) were mixed. Immunoprecipitations were undertaken employing an anti-GFP antibody and electrophoresed on an SDS/polyacrylamide gel, which was stained with Colloidal Blue (**A**). Migration of the LRRK2 band is indicated with an arrowhead and the GFP band is indicated with an arrow. Molecular-mass markers (kDa) are indicated on the left-hand side of the gels. The entire lane from each gel was excised, digested with trypsin and processed for MS. Each sample was analysed with Orbitrap MS and quantified using MaxQuant (version 13.13.10) [34] and a summary of results are presented in the Tables on the right-hand side. The number of peptides and percentage of sequence coverage corresponding to the indicated protein which were quantified are shown along with the ratios of enrichment for labelled compared with unlabelled peptides (Ratio H/L) for each comparison of GFP with wild-type LRRK2 (**A**) and GFP with LRRK2(G2019S) (**B**). The posterior error probability (PEP) is shown, which measures the accuracy of MaxQuant quantification where the closer to zero, the higher the probability of specific interaction [34].

and specific activity is represented as c.p.m./independent density values.

Affinity purification of 14-3-3 with a di-phosphorylated peptide encompassing Ser^{910} and Ser^{935}

An N-terminally biotinylated di-phosphorylated peptide encompassing Ser^{910} and Ser^{935} (biotin–KKKSNpSISVGEFYRDAVLQRCSPNLQRHSNpSLGPIF) was conjugated to streptavidin–agarose (1 μg peptide/μg of agarose). Aliquots of agarose beads (10 μl) were treated with or without λ phosphatase for 30 min at 30 °C, with λ phosphatase being in the presence or absence of 50 mM EDTA. Conjugated beads were then incubated with 3 mg of HEK-293 cell lysate at 4 °C for 1 h. Following two washes with lysis buffer supplemented with 0.5 M NaCl, beads were boiled in LDS sample buffer and samples subjected to immunoblot analysis for 14-3-3.

Fluorescence microscopy

HEK-293 Flp-in T-REx cells harbouring GFP-tagged LRRK2 and the PD-associated mutations were plated in four-well glass bottomed CC2-coated chamber slides (Nunc). After plating (1 day), cells were induced with 1 μg/ml doxycycline and 24 h later, cells were fixed in 4 % (w/v) paraformaldehyde buffered in PBS (pH 7.0–7.6) (purchased from USB, #19943). Cells were mounted in ProLong Gold (Invitrogen) and imaged under the same settings for each mutant with a Zeiss LSM 700 confocal microscope using an α-Plan-Apochromat $\times$100 objective.

RESULTS

Association of LRRK2 with 14-3-3

We employed quantitative SILAC-based MS to identify proteins associated with immunoprecipitates of stably expressed full-length GFP–LRRK2 (Figure 1A), as well as the GFP–LRRK2(G2019S) mutant (Figure 1B), derived from HEK-293 cells. The top hits, which were enriched at 10–30-fold higher levels with GFP–LRRK2 or GFP–LRRK2(G2019S) compared with GFP alone, comprised various isoforms of 14-3-3 (Figure 1). The two other major interactors observed were two isoforms of the Hsp90 chaperone associated with its kinase-specific targeting CDC37 (cell division cycle 37) subunit (enriched 5–15-fold). Hsp90 and CDC37 associated with both wild-type LRRK2 and

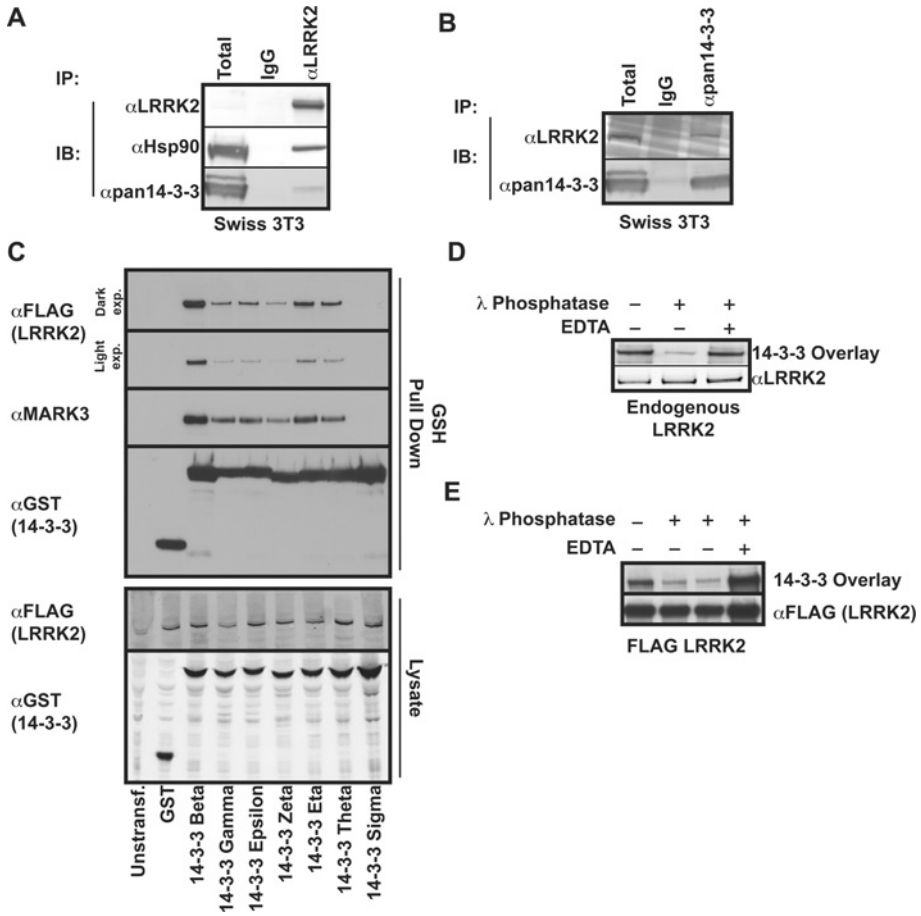

Figure 2 Characterization of 14-3-3 and LRRK2 interaction

(**A**) Swiss 3T3 lysate (5 mg) was subjected to immunoprecipitation (IP) with control IgG or anti-LRRK2(S348C) antibody. Immunoprecipitates were subjected to immunoblot (IB) analysis with the indicated antibodies (α). (**B**) Swiss 3T3 lysate (5 mg) was subjected to immunoprecipitation with anti-pan-14-3-3 antibodies and immunoprecipitates were immunoblotted with the indicated antibodies. (**C**) T-REx HEK 293 cells stably expressing FLAG–LRRK2 [11] were transfected with pEBG plasmids encoding GST (glutathione transferase) or the indicated GST-tagged isoform of 14-3-3 and induced to express LRRK2 by inclusion of 1 μg/ml doxycycline in the culture medium. Post-transfection (36 h), cells were lysed and glutathione–Sepharose affinity-purified proteins were immunoblotted with the indicated antibodies. (**D**) Endogenous LRRK2 was immunoprecipitated from Swiss 3T3 cells with anti-LRRK2(S348C) and subsequently treated with λ phosphatase in the absence or presence of EDTA prior to immunoblot analysis with the indicated antibodies or a 14-3-3 overlay assay. (**E**) As in (**D**), except that the experiment was undertaken with immunoprecipitated FLAG–LRRK2 obtained following transient transfection in HEK-293 cells.

the LRRK2(G2019S) mutant, and have been reported previously to interact with LRRK2 [15]. No other significant interactors of LRRK2 were detected in this screen.

We found that endogenous 14-3-3, as well as Hsp90, was co-immunoprecipitated with endogenous LRRK2 from Swiss 3T3 cells (Figure 2A). We also observed that endogenous LRRK2 was co-immunoprecipitated with an antibody that recognizes endogenous 14-3-3 isoforms from Swiss 3T3 cells (Figure 2B). Plasmids encoding expression of seven isoforms of human 14-3-3 were transfected into HEK-293 cells stably expressing full-length FLAG–LRRK2. Following affinity purification, apart from the atypical σ isoform, all other isoforms of 14-3-3 interacted with FLAG–LRRK2 (Figure 2C). As a control we also demonstrated that all 14-3-3 isoforms except 14-3-3σ interacted with endogenous MARK3, a previously characterized 14-3-3 interactor [16].

14-3-3 isoforms mostly interact with specific phosphorylated residues on their binding partners [17,18]. To verify whether association of 14-3-3 with LRRK2 was dependent on phosphorylation, we incubated endogenous LRRK2 (Figure 2D) or overexpressed FLAG–LRRK2 (Figure 2E) in the presence or absence of λ phosphatase. λ phosphatase markedly reduced interaction of 14-3-3 with LRRK2 assessed using the overlay assay. This effect was suppressed by the inclusion of the λ phosphatase inhibitor EDTA in the assay (Figures 2D and 2E). Residual binding of 14-3-3 to LRRK2 following λ phosphatase treatment is presumably due to incomplete dephosphorylation of LRRK2.

Mapping of major phosphorylation sites on endogenous LRRK2

To determine which phosphorylated residue(s) mediate binding to 14-3-3, we performed detailed phospho-peptide Orbitrap MS analysis of endogenous LRRK2 immunoprecipitated from mouse Swiss 3T3 cells (Figure 3A). This revealed three clear phosphorylation sites, namely Ser^{860}, Ser^{910} and Ser^{935} (Figure 3B). These residues lie in the N-terminal non-catalytic region of LRRK2 just prior to the leucine-rich repeats (Figure 3C). We also analysed phosphorylation of overexpressed full-length human FLAG–LRRK2 expressed in HEK-293 cells, which confirmed that Ser^{860}, Ser^{910} and Ser^{935} were major sites of phosphorylation (Figures 3A and 3B). In addition, we found three

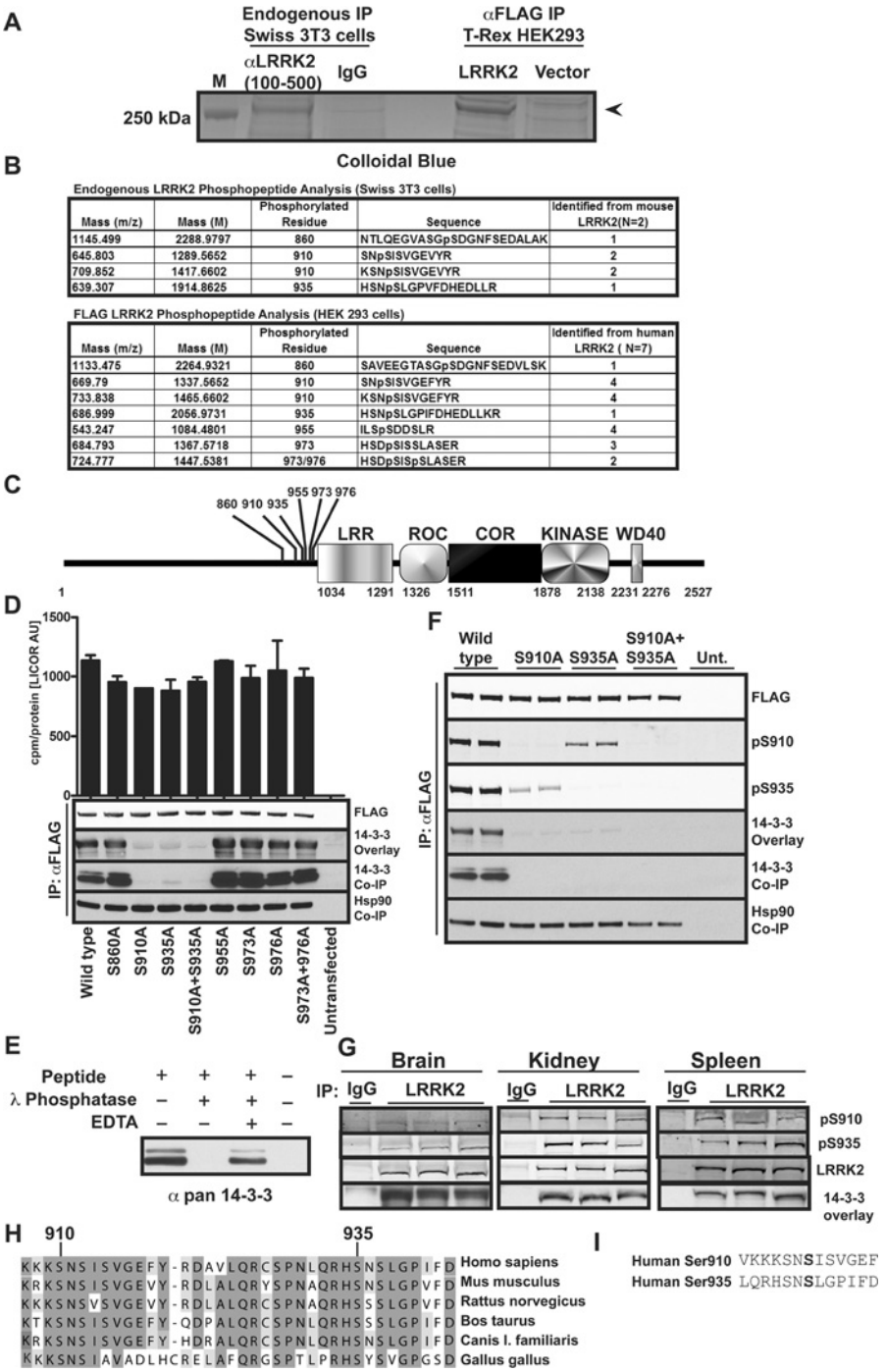

Figure 3 Ser^{910} and Ser^{935} phosphorylation mediate binding of LRRK2 to 14-3-3

(**A**) Endogenous LRRK2 was immunoprecipitated (IP) with anti-LRRK2-(100–500) (S348C) antibody from Swiss 3T3 cells and FLAG–LRRK2 was immunoprecipitated with anti-FLAG–agarose from stable inducible T-REx HEK-293 cells. Immunoprecipitates were subjected to electrophoresis on a 4–12 % Novex SDS/polyacrylamide gel and stained with Colloidal Blue. The gel is representative of several experiments. LRRK2 tryptic peptides were subjected to LC-MS/MS on an LTQ-Orbitrap mass spectrometer. M, molecular-mass marker. (**B**) Phospho-peptides identified by LTQ-Orbitrap MS shown in tabular format. Observed mass (*m*/*z*) and predicted mass (M) are shown, and the site of phosphorylation and peptide sequence are identified. The number of experiments evaluated (*N*) is indicated at the top of the column and the number of times, in total, the phosphorylated peptide was identified is indicated. (**C**) Domain structure of LRRK2 is presented to scale, with amino acid residues indicating domain boundaries indicated. Positions of identified phosphorylation sites are shown. LRR, leucine-rich repeat. (**D**) The indicated phosphorylation sites identified in (**A**) and (**B**) were mutated to an alanine residue and transiently expressed in HEK-293 cells. LRRK2 was immunoprecipitated with anti-FLAG–agarose and equal amounts of each protein were probed with FLAG (total) and the ability to directly bind 14-3-3 was assessed in an overlay assay. 14-3-3 and Hsp90 co-immunoprecipitation (Co-IP) was determined by immunoblotting the immunoprecipitates with the indicated antibodies. Kinase activity was assayed against 30 μM Nictide and specific activity was determined by correcting incorporation of phosphate for protein levels in the immunoprecipitate by quantitative immunoblot using the Odyssey system and is presented as c.p.m./absorbance units (cpm/LICOR AU). The data are the average for duplicate experiments that were repeated four separate times with similar results. (**E**) Streptavidin–agarose was conjugated to a biotinylated di-phosphorylated peptide encompassing Ser^{910} (pS910) and Ser^{935} (pS935) and incubated in the presence or absence of λ phosphatase in the presence or absence of the EDTA phosphatase inhibitor. The agarose beads were then incubated with HEK-293 cell lysates and interaction of 14-3-3 was assessed after beads were extensively washed and subjected to 14-3-3 immunoblot analysis. (**F**) The indicated forms of FLAG–LRRK2 were expressed in HEK-293 cells by transient transfection.

other phosphorylation sites in the overexpressed human FLAG–LRRK2 preparation, namely Ser^{955}, Ser^{973} and Ser^{976} (Figures 3B and 3C). The phospho-peptides encompassing Ser^{955}, Ser^{973} and Ser^{976} were also detected in our analysis of endogenous LRRK2, but owing to the lower abundance of these peptides, we were unable to assign the exact phosphorylation sites (results not shown).

Phosphorylation of Ser^{910} and Ser^{935} mediates 14-3-3 binding, but does not control kinase activity

We observed that mutation of Ser^{860}, Ser^{955}, Ser^{973}, Ser^{976} or both Ser^{973}/Ser^{976} phosphorylation sites to an alanine residue did not affect binding of 14-3-3 to full-length FLAG–LRRK2 (Figure 3D). Strikingly, however, mutation of Ser^{910} and/or Ser^{935} to an alanine residue abolished 14-3-3 interaction, indicating that phosphorylation of both of these residues is necessary for binding of LRRK2 to 14-3-3 isoforms (Figure 3D). Mutation of Ser^{910} and/or Ser^{935} or any of the other identified phosphorylation sites did not affect LRRK2 protein kinase activity (Figure 3D). To study whether phosphorylation of Ser^{910} and Ser^{935} was sufficient to mediate interaction with 14-3-3 isoforms, we generated a di-phosphorylated biotinylated peptide encompassing Ser^{910} and Ser^{935}. We observed that when this was conjugated to streptavidin–agarose, it efficiently affinity-purified 14-3-3 isoforms from HEK-293 cell extracts (Figure 3E). Incubation of this peptide with λ phosphatase to dephosphorylate Ser^{910} and Ser^{935} prevented interaction with 14-3-3 isoforms, an effect that was not observed when the λ phosphatase inhibitor EDTA was included (Figure 3E).

Generation of Ser^{910} and Ser^{935} phospho-specific antibodies

We next generated phospho-specific antibodies recognizing LRRK2 phosphorylated at Ser^{910} or Ser^{935}. These antibodies were specific, as mutation of Ser^{910} to an alanine residue ablated recognition of LRRK2 with an anti-phospho-Ser^{910} antibody and, similarly, mutation of Ser^{935} abolished recognition with the anti-phospho-Ser^{935} antibody (Figure 3F). We consistently observed that mutation of Ser^{910} to an alanine residue reduced phosphorylation of Ser^{935} approx. 2-fold and the similar mutation of Ser^{935} reduced phosphorylation of Ser^{910} approx. 2-fold as quantified by the Odyssey system (Figure 3F). Utilizing these antibodies, we demonstrate that endogenous LRRK2 immunoprecipitated from mouse brain, kidney and spleen was phosphorylated at Ser^{910}, as well as Ser^{935}, and also bound 14-3-3 (Figure 3G).

Sequence alignments indicate that the Ser^{910} and Ser^{935} sites, as well as residues surrounding them, are highly conserved in mammalian species (Figure 3H). This region encompassing Ser^{910} and Ser^{935} is not present in *Caenorhabditis elegans* or *Drosophila melanogaster* LRK-1, or, indeed, mammalian LRRK1. Comparison of the residues surrounding Ser^{910} and Ser^{935} indicates some striking similarities (Figure 3I, i.e. basic residues at the −3 and −4 positions, a serine residue at the −2 position, an asparagine residue at the −1 position and a large hydrophobic residue at the +1 position).

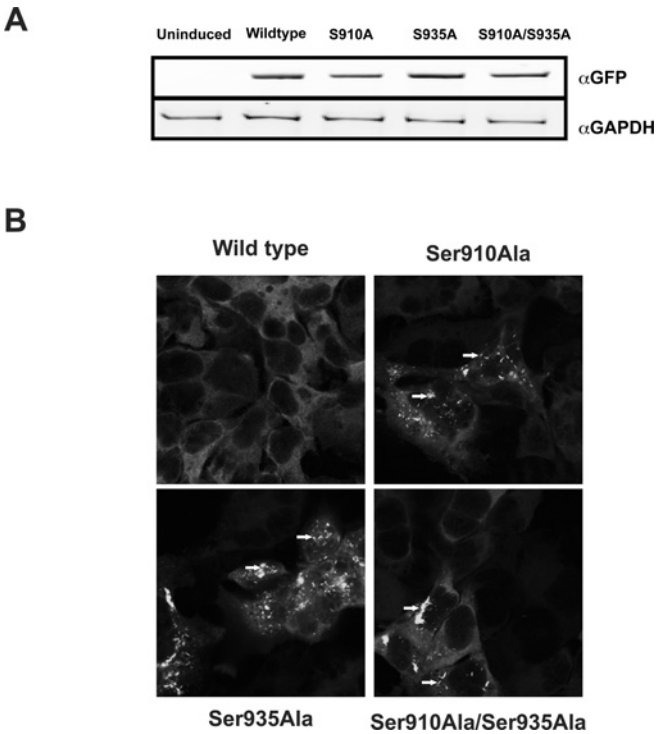

Figure 4 14-3-3 binding influences LRRK2 cytoplasmic localization

(**A**) Stable inducible T-REx cells lines harbouring the indicated forms of LRRK2 were induced for 24 h with 0.1 μg/ml doxycycline to induce expression of GFP–LRRK2. Equal amounts of cell lysate from induced cells of each mutant were subjected to immunoblot analysis with anti-GFP antibodies to detect the fusion protein or anti-GAPDH (glyceraldehyde-3-phosphate dehydrogenase) antibodies as a loading control. (**B**) Fluorescent micrographs representative of cultures of the indicated forms GFP–LRRK2 are shown. Cytoplasmic pools of GFP–LRRK2 observed in the non-14-3-3-binding mutants are indicated with white arrows.

Disruption of 14-3-3 binding induces accumulation of LRRK2 within cytoplasmic pools resembling inclusion bodies

A common role of 14-3-3 proteins is to influence the subcellular localization of the protein to which it binds. We therefore studied whether 14-3-3 binding might affect LRRK2 cellular localization. To ensure low-level expression and as uniform as possible, we generated Flp-in T-REx 293 cells that stably express the wild-type and non-14-3-3-binding Ser^{910}/Ser^{935} mutant forms of full-length GFP–LRRK2. Immunoblot analysis revealed that the wild-type and mutant GFP–LRRK2 forms were expressed at similar levels (Figure 4A). We next studied the cellular localization using confocal microscopy and found that, consistent with a previous report [19], wild-type LRRK2 was uniformly distributed throughout the cytosol and excluded from the nucleus (Figure 4B). In contrast, the non-14-3-3-binding LRRK2(S910A), LRRK2(S935A) and LRRK2(S910A/S935A) mutants accumulated within cytosolic pools resembling inclusion bodies (Figure 4B).

Post-transfection (36 h), these were immunoprecipitated with anti-FLAG antibody and immunoblotted with phospho-specific antibodies against Ser^{910} (S357C) and Ser^{935} (S814C). Direct binding of immunoprecipitates to 14-3-3 was also assessed by a 14-3-3 overlay assay and co-immunoprecipitation of 14-3-3 and Hsp90 was assessed by immunoblotting with the respective antibodies. Unt., untransfected. (**G**) LRRK2 was immunoprecipitated from tissues of wild-type male C57BL/6 mice and immunoblotted for Ser^{910} and Ser^{935} phosphorylation and 14-3-3 binding was assessed by overlay assay as in (**F**). (**H**) Multiple sequence alignment of LRRK2 from *Homo sapiens* (NP_940980), *Pan troglodytes* (XP_001168494), *Mus musculus* (NP_080006), *Rattus norvegicus* (XP_235581), *Bos taurus* (XP_615760), *Canis lupus familiaris* (XP_543734) and *Gallus gallus* (XP_427077). Positions of the phosphorylated residues Ser^{910} and Ser^{935} are indicated. Identical residues are indicated in grey. (**I**) Sequence comparison of residues surrounding the Ser^{910} and Ser^{935} phosphorylation sites of human LRRK2.

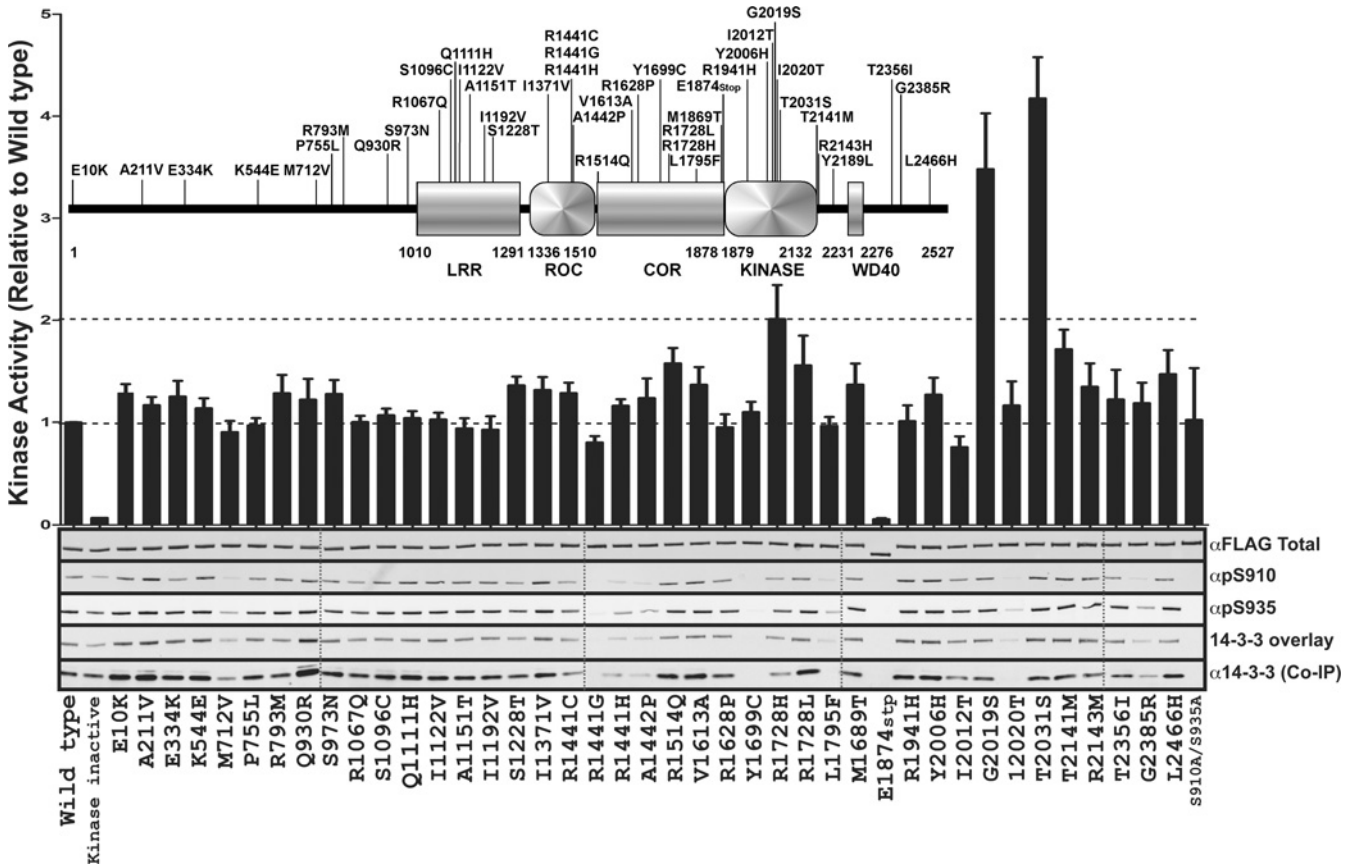

Figure 5 Activity and 14-3-3 binding of 41 PD-associated LRRK2 mutants

The inset shows the domain structure of LRRK2 with the leucine-rich repeats (LRR), ROC domain, COR domain, kinase catalytic domain (KINASE) and the minimal WD40 repeat domain (WD40) annotated. Positions of the PD-associated mutations are shown. The amino acid boundaries of the domains are indicated. The indicated variants of full-length FLAG-tagged LRRK2 were transiently expressed in HEK-293 cells and subjected to immunoprecipitation analysis. Kinase activity of immunoprecipitates was assessed against LRRKtide and specific activity was determined by quantitative anti-FLAG immunoblot analysis of LRRK2 using the Odyssey system and was defined as c.p.m./absorbance unit. Wild-type LRRK2 activity was set to 1 and the mutant activities are relative to wild-type. Assays were performed in duplicate, for three experiments, and expressed as the means ± S.E.M. FLAG–LRRK2 immunoprecipitates were also subjected to immunoblot analysis with anti-FLAG, anti-phospho-Ser^{910} (pS910) and anti-phospho-Ser^{935} (pS935) antibodies. 14-3-3 binding to the LRRK2 variants was assessed by 14-3-3 far-Western blot analyses and 14-3-3 immunoblotting for co-precipitating (Co-IP) 14-3-3.

Characterization of 14-3-3 binding of 41 LRRK2 PD-associated mutants

We next decided to investigate the Ser^{910}/Ser^{935} phosphorylation and 14-3-3-binding properties of 41 PD forms of LRRK2. These mutations include the six most common pathogenic mutations that have been described to date (R1441C, R1441G, R1441H, Y1699C, G2019S and I2020T) [5,6]. Most of the other mutations studied have only been observed in low numbers of PD patients and further work is required to assess the contributions these mutations make to the development of disease [6]. The location of different mutations in LRRK2 analysed is indicated in the Figure 5 (inset). We expressed full-length wild-type and mutant forms of LRRK2 with an N-terminal FLAG epitope tag in HEK-293 cells. LRRK2 was immunoprecipitated and levels of protein were determined by quantitative immunoblotting analysis (Odyssey system). Similar levels of LRRK2 forms were subjected to immunoblot analysis, which revealed that most of the mutants were phosphorylated at Ser^{910} and Ser^{935} to a similar extent as the wild-type enzyme and interacted with 14-3-3 (Figure 5, lower panel). However, Ser^{910}/Ser^{935} phosphorylation and hence 14-3-3 binding were abolished in four mutants (R1441G, Y1699C, E1874stop and I2020T) (Figure 5, lower panel). Phosphorylation of Ser^{910}/Ser^{935} and 14-3-3 binding were significantly reduced in six other mutants (M712V, R1441H, R1441C, A1442P, L1795F and G2385R) (Figure 5, lower panel).

We also compared the relative protein kinase specific activity of the 41 mutant forms of LRRK2 employing the LRRKtide peptide substrate [10] (Figure 5). Consistent with previous work [8–10], the LRRK2(G2019S) mutant possessed approx. 3-fold higher specific activity than wild-type LRRK2. Two other mutants, LRRK2(R1728H) and LRRK2(T2031S), also exhibited 2- and 4-fold increased activity respectively compared with wild-type LRRK2. Apart from the R1874stop mutation that lacks the kinase domain and is therefore inactive, all other mutants tested possessed similar activity to wild-type LRRK2.

Association of 14-3-3 with endogenous LRRK2 is impaired in LRRK2(R1441C) knock-in mice

To obtain further evidence that the LRRK2(R1441C) PD mutation disrupts 14-3-3 binding, we compared levels of 14-3-3 associated with endogenous LRRK2 derived from previously reported littermate wild-type and homozygous LRRK2(R1441C) knock-in mice [20]. LRRK2 was immunoprecipitated from spleen, kidney and brain from three separate mice of each genotype. Immunoblotting and 14-3-3 overlay analysis demonstrated that

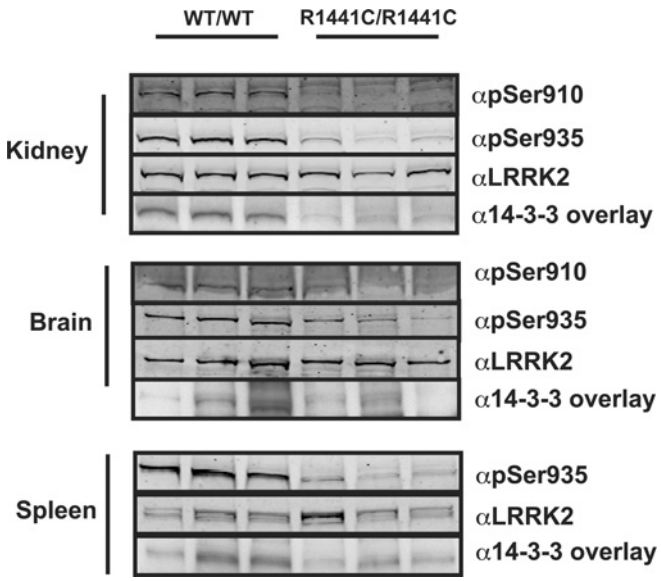

Figure 6 Disruption of Ser^{910}/Ser^{935} phosphorylation and 14-3-3 binding in LRRK2(R1441C) knock-in mice

Brain, kidney and spleen tissue were rapidly excised from three homozygous LRRK2(R1441C) knock-in mice and three wild-type littermate controls and snap-frozen in liquid nitrogen. LRRK2 was immunoprecipitated from whole-tissue lysate of brain, kidney or spleen. Immunoprecipitates were immunoblotted for phosphorylation of LRRK2 at Ser^{910} and Ser^{935} and for total LRRK2. The ability to interact with 14-3-3 binding was assessed by 14-3-3 far-Western blot analysis. Note insufficient sample from spleen was available for measuring Ser^{910} phosphorylation.

level of LRRK2 expression was similar in the wild-type and knock-in mice, however, the level of Ser^{910}/Ser^{935} phosphorylation and associated 14-3-3 was markedly reduced in tissues derived from LRRK2(R1441C) knock-in mice compared with wild-type (Figure 6). The largest effect of the knock-in mutation was observed in kidney.

Cellular localization of 41 mutant forms of LRRK2

To ensure low-level expression and as uniform as possible of the wild-type and mutant forms of full-length GFP–LRRK2, we generated the Flp-in T-REx 293 cells that stably express the wild-type and mutant forms of GFP–LRRK2. Immunoblot analysis revealed that GFP–LRRK2 forms were expressed at relatively similar levels (Figure 7). The localization of wild-type, kinase-dead and many other LRRK2 mutants studied were uniformly distributed throughout the cytosol and excluded from the nucleus with no accumulation within cytoplasmic pools observed (Figure 7 and Supplementary Figure S1 to view larger images at http://www.BiochemJ.org/bj/430/bj4300393add.htm). Strikingly, most mutants that displayed reduced Ser^{910}/Ser^{935} phosphorylation and binding to 14-3-3 accumulated within cytosolic pools resembling inclusion bodies (R1441C, R1441G, R1441H, A1442P, Y1699C, L1795F and I2020T). Not counting the truncated E1874stop mutant, which displays diffuse cytoplasmic localization, only two other mutants (M712V and G2385R) displaying reduced Ser^{910}/Ser^{935} phosphorylation and 14-3-3 binding (Figure 5), but did not accumulate in cytoplasmic pools (Figure 7 and Supplementary Figure S1). It is possible that the ability of these mutants to still interact weakly with 14-3-3 isoforms may prevent their accumulation within cytoplasmic pools. Only a single mutant (R1067Q) was found to interact with 14-3-3 and accumulate within cytoplasmic pools (Figure 7 and Supplementary Figure S1). The reasons for this require further work.

DISCUSSION

In the present study we have established that 14-3-3 isoforms interact with endogenous LRRK2 and this is mediated by phosphorylation of Ser^{910} and Ser^{935}. The finding that a di-phosphorylated peptide encompassing Ser^{910} and Ser^{935} interacted with 14-3-3 isoforms in HEK-293 cell extracts and that LRRK2 S910A/S935A do not interact with 14-3-3 suggests that phosphorylation of these residues is necessary and sufficient to enable LRRK2 to interact with 14-3-3 isoforms. 14-3-3 proteins interact dynamically with many intracellular proteins, exerting widespread influence on diverse cellular processes. They operate by binding to specific phosphorylated residues on target proteins. The finding that LRRK2 interacts with 14-3-3 isoforms could not be predicted by analysis of the primary sequence, because the residues surrounding the phosphorylation sites at positions 910 and 935 do not adhere to the optimal mode 1 and 2 consensus binding motifs for a common mode of 14-3-3 interaction [17,18]. However, many proteins that interact with 14-3-3 do so via diverse non-predictable atypical binding motifs, presumably because other structural features contribute to the interactions [17].

Our data suggest that phosphorylation of both Ser^{910} and Ser^{935} is required for stable interaction of 14-3-3 with LRRK2, as mutation of either Ser^{910} or Ser^{935} abolishes 14-3-3 interaction. 14-3-3 molecules form dimers with each monomer having the ability to interact with a phosphorylated residue [18]. Thus a 14-3-3 dimer has the capacity to interact with two phosphorylated residues. It is possible that one dimer of 14-3-3 interacts with both phosphorylated Ser^{910} and phosphorylated Ser^{935}. We also observed that mutation of either Ser^{910} or Ser^{935} to an alanine residue induced a significant dephosphorylation of the other residue (Figure 3F). This could be explained if 14-3-3 binding protected Ser^{910} and Ser^{935} from becoming dephosphorylated by a protein phosphatase. Thus abolishing 14-3-3 binding by mutation of either Ser^{910} or Ser^{935} would promote dephosphorylation of the other site. 14-3-3 binding to other targets such as phosphoinositide 4-kinase IIIβ [21] or CDC25C [22] protects these enzymes from dephosphorylation, presumably by sterically shielding phosphorylated residues from protein phosphatases.

14-3-3 proteins were originally identified 42 years ago as acidic proteins that were highly expressed in the brain [23]. Since then 14-3-3 proteins have been implicated in the regulation of numerous neurological disorders including PD [24,25]. For example, 14-3-3η binds to parkin, a protein mutated in autosomal recessive juvenile parkinsonism, and negatively regulates its E3 ligase activity [26]. 14-3-3 proteins interact with α-synuclein [27] and have been found in Lewy bodies in brains of patients with PD [28]. Additionally, 14-3-3θ, 14-3-3ε and 14-3-3γ were recently shown to suppress the toxic effects of α-synuclein overexpression in a cell-based model of neurotoxicity [29]. Our data suggest that 14-3-3 binding to LRRK2 may be relevant to PD, as, strikingly, ten out of 41 mutations studied displayed reduced phosphorylation of Ser^{910}/Ser^{935} and binding to 14-3-3 isoforms.

How 14-3-3 interaction influences LRRK2 function requires further investigation. Our data suggest that this interaction does not control LRRK2 protein kinase activity, as mutation of Ser^{910} and/or Ser^{935} does not influence LRRK2 catalytic activity (Figure 3D). However, our experiments indicate that 14-3-3 binding influences the cytoplasmic localization of LRRK2, as disruption of 14-3-3 binding by mutation of Ser^{910}/Ser^{935} caused

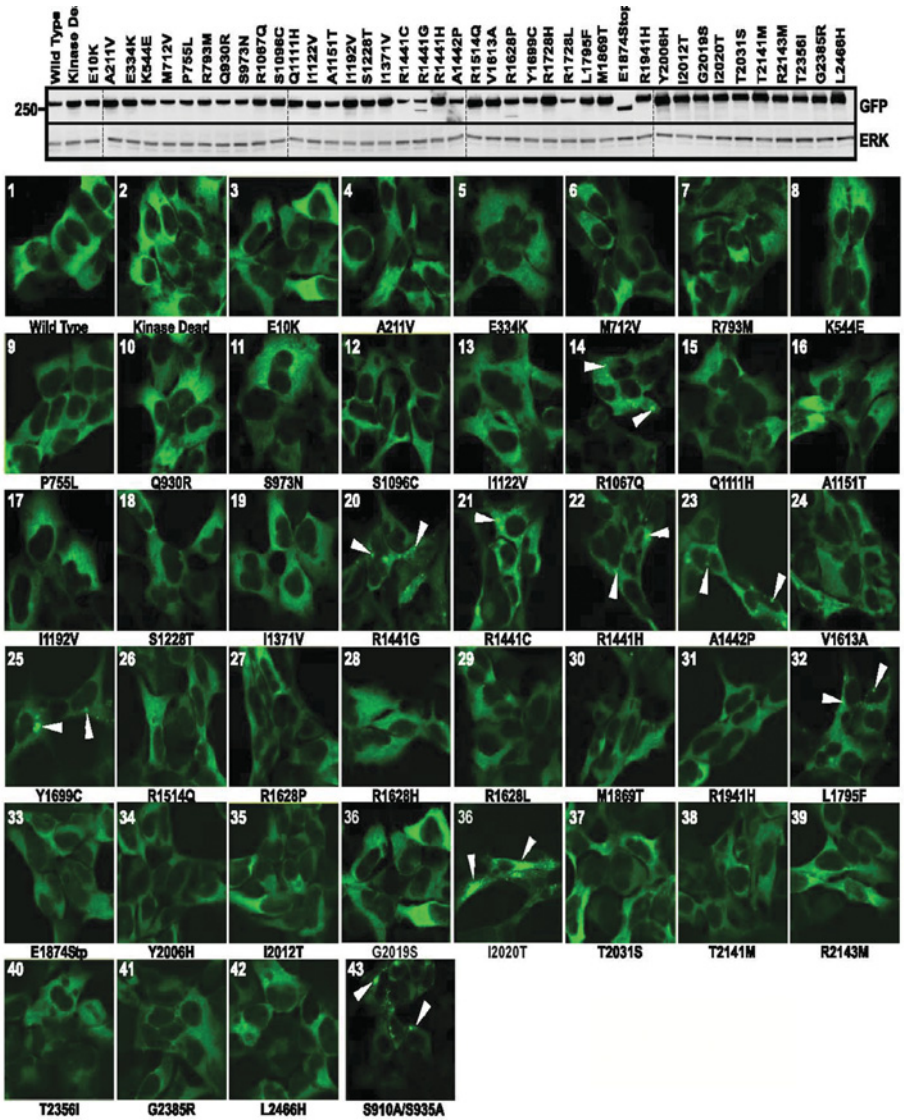

Figure 7 Localization of 41 PD-associated LRRK2 mutants

Parallel cultures of stable inducible T-REx cells lines harbouring the indicated mutations were induced for 24 h with 1 μg/ml doxycycline to induce expression of GFP–LRRK2. Upper panel, equal amounts of cell lysate from induced cells of each mutant were subjected to immunoblot analysis with anti-GFP antibodies to detect the fusion protein or anti-ERK1 (extracellular-signal-regulated kinase 1) antibodies as a loading control. The molecular mass is indicated on the left-hand side (kDa). Lower panel, fluorescent micrographs representative of cultures of each PD-associated mutant (panels 1–43) are shown. Cytoplasmic pools of GFP–LRRK2 are indicated with white arrowheads. Localization analyses were performed in duplicate, on two independently generated stable cell lines. Larger panels of each of the micrographs shown are presented in Supplementary Figure S1 at http://www.BiochemJ.org/bj/430/bj4300393add.htm).

LRRK2 to accumulate within cytoplasmic pools. Previous work has revealed that LRRK2 mutants, including LRRK2(R1441C) and LRRK2(Y1699C), when expressed in cells accumulate within cytoplasmic pools resembling inclusion bodies [9,19,30], a finding we were able to confirm in the present study (Figure 7 and Supplementary Figure S1). These cytoplasmic pools were suggested to comprise aggregates of misfolded unstable LRRK2 protein [9]. If this were the case, it may suggest that 14-3-3 plays a role in stabilizing LRRK2. Strikingly, five out of the six most common pathogenic mutations (R1441C, R1441G, R1441H, Y1699C and I2020T) accumulated within cytoplasmic pools and displayed reduced Ser^{910}/Ser^{935} phosphorylation and binding to 14-3-3 under conditions in which wild-type LRRK2 and most other LRRK2 mutants analysed bound 14-3-3 and did not accumulate within cytosolic pools (Figure 7). We also validate these findings by demonstrating that Ser^{910}/Ser^{935} phosphorylation and 14-3-3 binding is markedly reduced in three mouse tissues derived from homozygous R1441C knock-in mice that display impaired dopaminergic neurotransmission [20]. Further work is required to establish why the R1441C, R1441G, R1441H, Y1699C and I2020T mutations disrupt phosphorylation of Ser^{910} and Ser^{935}, hence inhibiting 14-3-3 binding. It is possible that these mutations are partially misfolded or unstable and are hence not properly recognized by the upstream protein kinase that phosphorylates the Ser^{910} and Ser^{935} residues.

In Supplementary Table S1 (at http://www.BiochemJ.org/bj/430/bj4300393add.htm) we subdivide the 41 LRRK2 mutations we have analysed into six groups on the basis of the impact that the mutations analysed in the present study have on protein kinase activity, Ser^{910}/Ser^{935} phosphorylation and 14-3-3-binding, as well as cellular localization. Only three out of the 41 mutations analysed markedly enhanced LRRK2 protein kinase

2–4-fold. Strikingly, the LRRK2(T2031S) mutation was more active than the LRRK2(G2019S) mutant, displaying nearly 4-fold higher activity than wild-type LRRK2. The LRRK2(T2031S) mutation has only been reported in a single Spanish patient with a family history of PD [31]. Interestingly, Thr^{2031} lies within the T-loop of the LRRK2 kinase domain, a region where many kinases are activated by phosphorylation. Recent studies have suggested that LRRK2 is capable of autophosphorylating itself at Thr^{2031} [32,33], although so far we have never been able to observe detectable phosphorylation of this site in endogenous or overexpressed LRRK2 by MS, perhaps indicating stoichiometry of phosphorylation of this residue is very low. We have found that changing Thr^{2031} to an alanine residue to prevent phosphorylation led to a similar increase in activity as the T2031S mutation (R.J. Nichols, unpublished work) and mutation to a glutamate residue to mimic phosphorylation inactivates LRRK2 (N. Dzamko, unpublished work). Further work is warranted to understand the role of Thr^{2031} and how its mutation to a serine residue and/or phosphorylation or other covalent modification affects LRRK2 catalytic activity. The LRRK2(R1728H) mutation displayed 2-fold increased kinase activity and was identified in a single patient with a family history of PD [6]. Arg^{1728} is located outside the kinase domain in the COR domain (Figure 5).

In future work it will be important to investigate further how 14-3-3 binding affects on LRRK2 stability, interaction with substrates or other regulators. It would also be interesting to undertake a more detailed characterization of the cytoplasmic pools resembling inclusion bodies that non-14-3-3-binding LRRK2 mutants accumulate in and to determine whether these do indeed comprise aggregates of misfolded protein. Our results analysing some of the properties of the 41 PD-associated forms of LRRK2 emphasize that most mutations do not exert their effects in the same way as the G2019S mutation by simply increasing catalytic activity. Finding out how the diverse mutations affect LRRK2 regulation, the ability to interact with binding partners and stability, as well as downstream functions, will provide valuable insights into how LRRK2 exerts its influence in PD. It would also be important to further explore links between LRRK2 Ser^{910}/Ser^{935} phosphorylation, 14-3-3 binding and its relevance to development of PD. However, as 28 LRRK2 mutations possessed similar activity, 14-3-3 binding and cellular localization as wild-type LRRK2, assuming that these comprise pathogenic mutations, there is clearly still much to learn about how the majority of the mutations described affect LRRK2 to cause PD. Finally, it would be interesting to undertake LRRK2 interactor screens from neuronal cell lines or brain tissues that might reveal cofactors other than 14-3-3 that would be relevant to understanding how LRRK2 is regulated and functions.

AUTHOR CONTRIBUTION

Jeremy Nichols and Nicolas Dzamko performed most of the experiments. Nicholas Morrice and David Campbell carried out the MS analysis. Maria Deak and Thomas Macartney carried out the cDNA cloning. Alban Ordureau performed the studies that contributed to the identification of the Ser^{910} phosphorylation site. Youren Tong and Jie Shen provided tissues from LRRK2(R1441C) knock-in mice. Alan Prescott supervised and performed the localization studies. Nicolas Dzamko, Jeremy Nichols and Dario Alessi planned the experiments, analysed the results and wrote the manuscript. Dario Alessi supervised the project.

ACKNOWLEDGEMENTS

We thank the Sequencing Service (School of Life Sciences, University of Dundee, Dundee, Scotland, U.K.) for DNA sequencing, the Post Genomics and Molecular Interactions Centre for Mass Spectrometry facilities (School of Life Sciences, University of Dundee, Dundee, Scotland, U.K.) and the protein production and antibody purification teams [Division of Signal Transduction Therapy (DSTT), University of Dundee, Dundee, Scotland, U.K.] co-ordinated by Hilary McLauchlan and James Hastie for purification of antibodies. We also thank Miratul Muqit for helpful discussions.

FUNDING

This work is supported by the Medical Research Council [Medical Research Council Technology (MRCT) Industry collaborative award to N.D.]; and The Michael J. Fox Foundation. The Division of Signal Transduction Therapy Unit is supported by the following pharmaceutical companies: AstraZeneca, Boehringer-Ingelheim, GlaxoSmithKline, Merck-Serono and Pfizer.

REFERENCES

1 Zimprich, A., Biskup, S., Leitner, P., Lichtner, P., Farrer, M., Lincoln, S., Kachergus, J., Hulihan, M., Uitti, R. J. and Calne, D. B. (2004) Mutations in LRRK2 cause autosomal-dominant parkinsonism with pleomorphic pathology. Neuron **44**, 601–607
2 Paisan-Ruiz, C., Jain, S., Evans, E. W., Gilks, W. P., Simon, J., van der Brug, M., Lopez de Munain, A., Aparicio, S., Gil, A. M., Khan, N. et al. (2004) Cloning of the gene containing mutations that cause PARK8-linked Parkinson's disease. Neuron **44**, 595–600
3 Mata, I. F., Wedemeyer, W. J., Farrer, M. J., Taylor, J. P. and Gallo, K. A. (2006) LRRK2 in Parkinson's disease: protein domains and functional insights. Trends Neurosci. **29**, 286–293
4 Healy, D. G., Falchi, M., O'Sullivan, S. S., Bonifati, V., Durr, A., Bressman, S., Brice, A., Aasly, J., Zabetian, C. P., Goldwurm, S. et al. (2008) Phenotype, genotype, and worldwide genetic penetrance of LRRK2-associated Parkinson's disease: a case-control study. Lancet Neurol. **7**, 583–590
5 Biskup, S. and West, A. B. (2009) Zeroing in on LRRK2-linked pathogenic mechanisms in Parkinson's disease. Biochim. Biophys. Acta **1792**, 625–633
6 Paisan-Ruiz, C., Nath, P., Washecka, N., Gibbs, J. R. and Singleton, A. B. (2008) Comprehensive analysis of LRRK2 in publicly available Parkinson's disease cases and neurologically normal controls. Hum. Mutat. **29**, 485–490
7 Anand, V. S. and Braithwaite, S. P. (2009) LRRK2 in Parkinson's disease: biochemical functions. FEBS J. **276**, 6428–6435
8 West, A. B., Moore, D. J., Biskup, S., Bugayenko, A., Smith, W. W., Ross, C. A., Dawson, V. L. and Dawson, T. M. (2005) Parkinson's disease-associated mutations in leucine-rich repeat kinase 2 augment kinase activity. Proc. Natl. Acad. Sci. U.S.A. **102**, 16842–16847
9 Greggio, E., Jain, S., Kingsbury, A., Bandopadhyay, R., Lewis, P., Kaganovich, A., van der Brug, M. P., Beilina, A., Blackinton, J., Thomas, K. J., Ahmad, R. et al. (2006) Kinase activity is required for the toxic effects of mutant LRRK2/dardarin. Neurobiol. Dis. **23**, 329–341
10 Jaleel, M., Nichols, R. J., Deak, M., Campbell, D. G., Gillardon, F., Knebel, A. and Alessi, D. R. (2007) LRRK2 phosphorylates moesin at threonine-558: characterization of how Parkinson's disease mutants affect kinase activity. Biochem. J. **405**, 307–317
11 Nichols, R. J., Dzamko, N., Hutti, J. E., Cantley, L. C., Deak, M., Moran, J., Bamborough, P., Reith, A. D. and Alessi, D. R. (2009) Substrate specificity and inhibitors of LRRK2, a protein kinase mutated in Parkinson's disease. Biochem. J. **424**, 47–60
12 Reed, S. E., Staley, E. M., Mayginnes, J. P., Pintel, D. J. and Tullis, G. E. (2006) Transfection of mammalian cells using linear polyethylenimine is a simple and effective means of producing recombinant adeno-associated virus vectors. J. Virol. Methods **138**, 85–98
13 Dubois, F., Vandermoere, F., Gernez, A., Murphy, J., Toth, R., Chen, S., Geraghty, K. M., Morrice, N. A. and Mackintosh, C. (2009) Differential 14-3-3-affinity capture reveals new downstream targets of PI 3-kinase signaling. Mol. Cell. Proteomics **8**, 2487–2499
14 Moorhead, G., Douglas, P., Cotelle, V., Harthill, J., Morrice, N., Meek, S., Deiting, U., Stitt, M., Scarabel, M., Aitken, A. and MacKintosh, C. (1999) Phosphorylation-dependent interactions between enzymes of plant metabolism and 14-3-3 proteins. Plant J. **18**, 1–12
15 Wang, L., Xie, C., Greggio, E., Parisiadou, L., Shim, H., Sun, L., Chandran, J., Lin, X., Lai, C., Yang, W. J. et al. (2008) The chaperone activity of heat shock protein 90 is critical for maintaining the stability of leucine-rich repeat kinase 2. J. Neurosci. **28**, 3384–3391
16 Goransson, O., Deak, M., Wullschleger, S., Morrice, N. A., Prescott, A. R. and Alessi, D. R. (2006) Regulation of the polarity kinases PAR-1/MARK by 14-3-3 interaction and phosphorylation. J. Cell Sci. **119**, 4059–4070
17 MacKintosh, C. (2004) Dynamic interactions between 14-3-3 proteins and phosphoproteins regulate diverse cellular processes. Biochem. J. **381**, 329–342
18 Yaffe, M. B., Rittinger, K., Volinia, S., Caron, P. R., Aitken, A., Leffers, H., Gamblin, S. J., Smerdon, S. J. and Cantley, L. C. (1997) The structural basis for 14-3-3:phosphopeptide binding specificity. Cell **91**, 961–971
19 Alegre-Abarrategui, J., Christian, H., Lufino, M. M., Mutihac, R., Venda, L. L., Ansorge, O. and Wade-Martins, R. (2009) LRRK2 regulates autophagic activity and localizes to specific membrane microdomains in a novel human genomic reporter cellular model. Hum. Mol. Genet. **18**, 4022–4034

20 Tong, Y., Pisani, A., Martella, G., Karouani, M., Yamaguchi, H., Pothos, E. N. and Shen, J. (2009) R1441C mutation in LRRK2 impairs dopaminergic neurotransmission in mice. Proc. Natl. Acad. Sci. U.S.A. **106**, 14622–14627
21 Hausser, A., Link, G., Hoene, M., Russo, C., Selchow, O. and Pfizenmaier, K. (2006) Phospho-specific binding of 14-3-3 proteins to phosphatidylinositol 4-kinase IIIβ protects from dephosphorylation and stabilizes lipid kinase activity. J. Cell Sci. **119**, 3613–3621
22 Hutchins, J. R., Dikovskaya, D. and Clarke, P. R. (2002) Dephosphorylation of the inhibitory phosphorylation site S287 in *Xenopus* Cdc25C by protein phosphatase-2A is inhibited by 14-3-3 binding. FEBS Lett. **528**, 267–271
23 Moore, B. W. and Perez, V. J. (1967) Specific acidic proteins of the nerous system. In Physiological and Biochemical Aspects of Nervous Integration (Carlson, F. D., ed.), pp. 343–359, Prentice-Hall, Woods Hole
24 Berg, D., Holzmann, C. and Riess, O. (2003) 14-3-3 proteins in the nervous system. Nat. Rev. Neurosci. **4**, 752–762
25 Chen, H. K., Fernandez-Funez, P., Acevedo, S. F., Lam, Y. C., Kaytor, M. D., Fernandez, M. H., Aitken, A., Skoulakis, E. M., Orr, H. T., Botas, J. and Zoghbi, H. Y. (2003) Interaction of Akt-phosphorylated ataxin-1 with 14-3-3 mediates neurodegeneration in spinocerebellar ataxia type 1. Cell **113**, 457–468
26 Sato, S., Chiba, T., Sakata, E., Kato, K., Mizuno, Y., Hattori, N. and Tanaka, K. (2006) 14-3-3η is a novel regulator of parkin ubiquitin ligase. EMBO J. **25**, 211–221
27 Ostrerova, N., Petrucelli, L., Farrer, M., Mehta, N., Choi, P., Hardy, J. and Wolozin, B. (1999) α-Synuclein shares physical and functional homology with 14-3-3 proteins. J. Neurosci. **19**, 5782–5791
28 Ubl, A., Berg, D., Holzmann, C., Kruger, R., Berger, K., Arzberger, T., Bornemann, A. and Riess, O. (2002) 14-3-3 protein is a component of Lewy bodies in Parkinson's disease-mutation analysis and association studies of 14-3-3η. Mol. Brain Res. **108**, 33–39
29 Yacoubian, T. A., Slone, S. R., Harrington, A. J., Hamamichi, S., Schieltz, J. M., Caldwell, G. A. and Standaert, D. G. (2010) Differential neuroprotective effects of 14-3-3 proteins in models of Parkinson's disease. Cell Death Dis. **1**, e2
30 Smith, W. W., Pei, Z., Jiang, H., Moore, D. J., Liang, Y., West, A. B., Dawson, V. L., Dawson, T. M. and Ross, C. A. (2005) Leucine-rich repeat kinase 2 (LRRK2) interacts with parkin, and mutant LRRK2 induces neuronal degeneration. Proc. Natl. Acad. Sci. U.S.A. **102**, 18676–18681
31 Lesage, S., Janin, S., Lohmann, E., Leutenegger, A. L., Leclere, L., Viallet, F., Pollak, P., Durif, F., Thobois, S., Layet, V. et al. (2007) LRRK2 exon 41 mutations in sporadic Parkinson disease in Europeans. Arch. Neurol. **64**, 425–430
32 Greggio, E., Taymans, J. M., Zhen, E. Y., Ryder, J., Vancraenenbroeck, R., Beilina, A., Sun, P., Deng, J., Jaffe, H., Baekelandt, V. et al. (2009) The Parkinson's disease kinase LRRK2 autophosphorylates its GTPase domain at multiple sites. Biochem. Biophys. Res. Commun. **389**, 449–454
33 Li, X., Moore, D. J., Xiong, Y., Dawson, T. M. and Dawson, V. L. (2010) Reevaluation of phosphorylation sites in the Parkinson's disease associated leucine rich repeat kinase-2. J. Biol. Chem., doi:10.1074/jbc.M110.127639
34 Cox, J. and Mann, M. (2008) MaxQuant enables high peptide identification rates, individualized p.p.b.-range mass accuracies and proteome-wide protein quantification. Nat. Biotechnol. **26**, 1367–1372

Received 31 March 2010/16 July 2010; accepted 19 July 2010
Published as BJ Immediate Publication 19 July 2010, doi:10.1042/BJ20100483

Biochem. J. (2010) **430**, 393–404 (Printed in Great Britain) doi:10.1042/BJ20100483

online data commentary

SUPPLEMENTARY ONLINE DATA

14-3-3 binding to LRRK2 is disrupted by multiple Parkinson's disease-associated mutations and regulates cytoplasmic localization

R. Jeremy NICHOLS*[1,3], Nicolas DZAMKO*, Nicholas A. MORRICE*[2], David G. CAMPBELL*, Maria DEAK*, Alban ORDUREAU*, Thomas MACARTNEY*, Youren TONG†, Jie SHEN†, Alan R. PRESCOTT‡ and Dario R. ALESSI*[3]

*MRC Protein Phosphorylation Unit, College of Life Sciences, University of Dundee, Dow Street, Dundee DD1 5EH, Scotland, U.K., †Center for Neurologic Diseases, Brigham and Women's Hospital, Program in Neuroscience, Harvard Medical School, Boston, MA 02115, U.S.A., and ‡Division of Cell Biology and Immunology, College of Life Sciences, University of Dundee, Dow Street, Dundee DD1 5EH, Scotland, U.K.

[1] Present address: Parkinson's Institute, 675 Almanor Ave., Sunnyvale, CA 94085, U.S.A.
[2] Present address: The Beatson Institute for Cancer Research, Garscube Estate, Switchback Road, Bearsden, Glasgow G61 1BD, Scotland, U.K.
[3] Correspondence may be addressed to either of these authors (jnichols@parkinsonsinstitute.org or d.r.alessi@dundee.ac.uk).

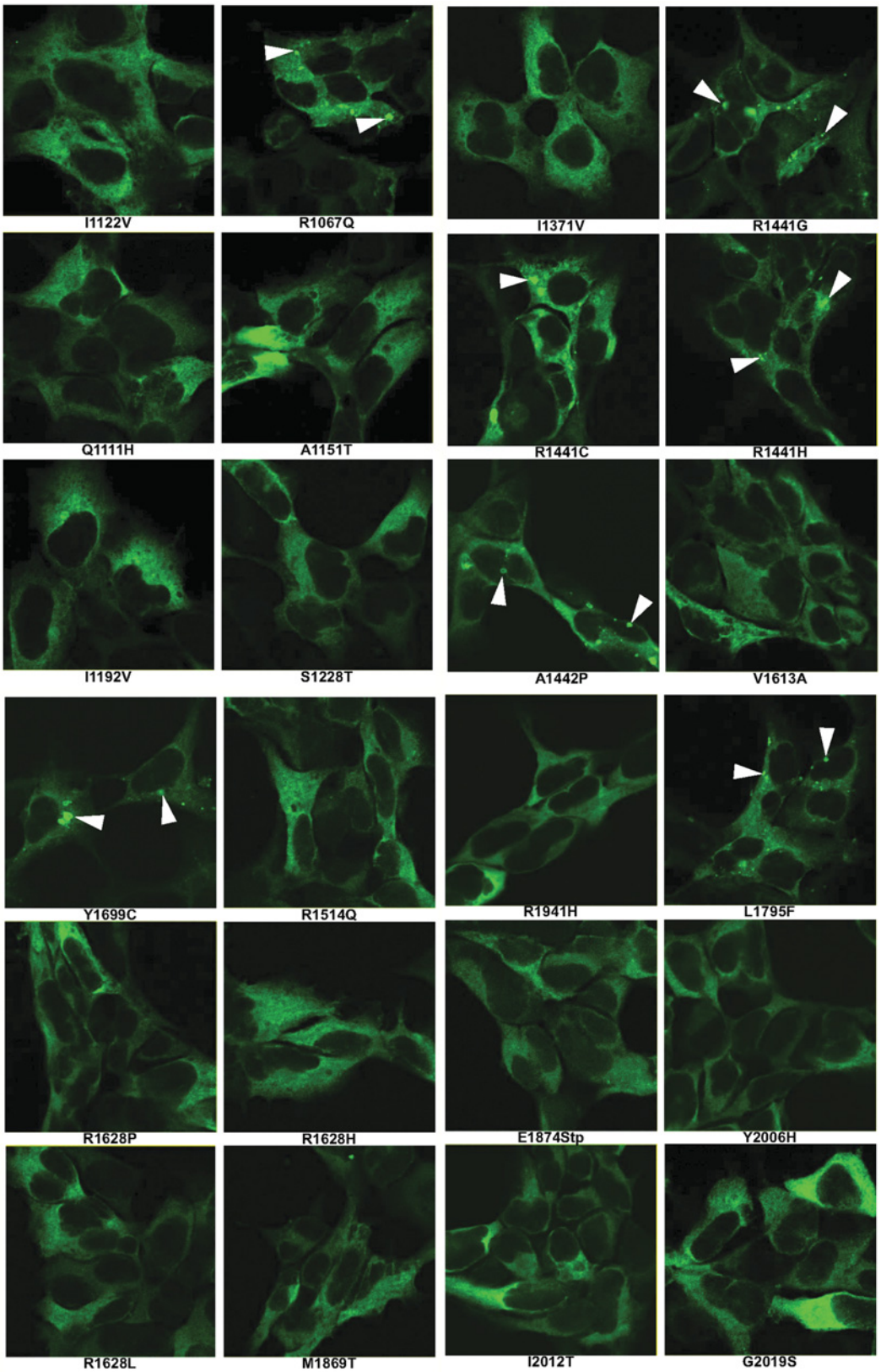

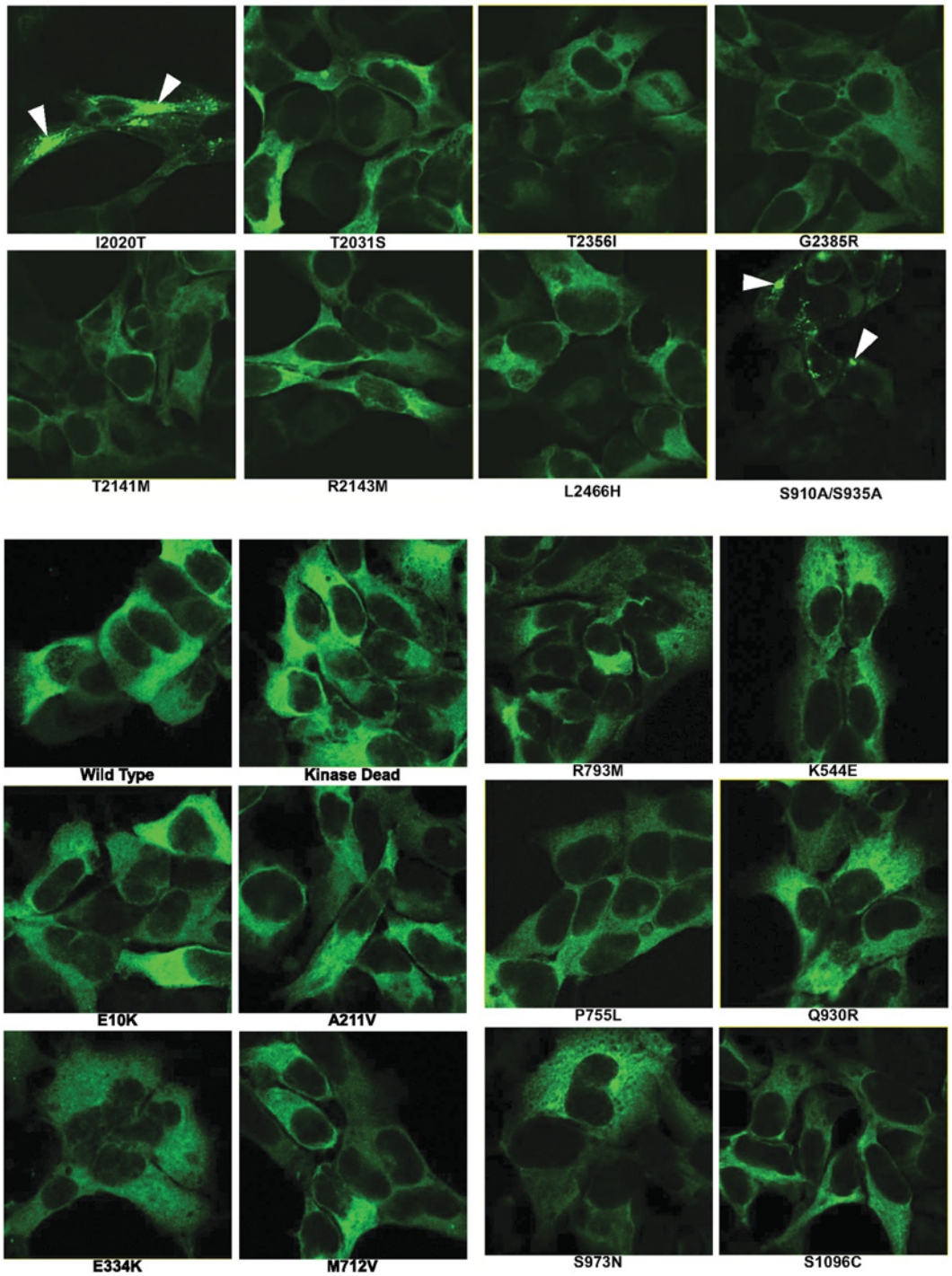

Figure S1 Localization of 41 PD-associated LRRK2 mutants

Micrographs are the same as those presented in Figure 6 of the main paper, except that each of the micrographs is larger to improve clarity.

Table S1 Summary of the effects of 41 PD-associated LRRK2 mutations

Kinase activity relative to wild-type, where 0 indicates no detectable activity, + equals approximately no change and each fold increase represented by and additional +. Effects of Ser^{910} and Ser^{935} phosphorylation and direct 14-3-3 binding, where no change is represented by ++, + indicates a decrease in Ser^{910}/Ser^{935} phosphorylation or 14-3-3 binding and - indicates no detectable Ser^{910}/Ser^{935} phosphorylation or 14-3-3 binding. Localization is denoted as diffuse for diffuse cytoplasmic staining. Aggregate denotes the appearance of cytoplasmic pools. We have divided LRRK2 mutants into six groups. Group 1 mutants display a >2-fold increase in kinase activity, but normal 14-3-3 binding and diffuse localization (green shading). Group 2 mutants display normal kinase activity but reduced Ser^{910}/Ser^{935} phosphorylation, as well as reduced 14-3-3 binding and accumulate within cytoplasmic pools (peach shading). Group 3 mutants display normal kinase activity, but reduced Ser^{910}/Ser^{935} phosphorylation, as well as reduced 14-3-3 binding and exhibit diffuse cytoplasmic localization (blue shading). The Group 4 mutant displays normal kinase activity, Ser^{910}/Ser^{935} phosphorylation and 14-3-3 binding but accumulates within cytoplasmic pools (yellow shading). The Group 5 mutant displays no kinase activity, Ser^{910}/Ser^{935} phosphorylation or 14-3-3 binding and localizes diffusely (red shading). Group 6 mutants display properties similar to wild-type LRRK2 (not shaded).

Mutant	Kinase activity	pSer910/pSer935	14-3-3 binding	Localization	Group
WT	+	++	++	Diffuse	
D2017A	0	++	++	Diffuse	
E10K	+	++	++	Diffuse	6
A211V	+	++	++	Diffuse	6
E334K	+	++	++	Diffuse	6
K544E	+	++	++	Diffuse	6
M712V	+	+	+	Diffuse	3
P755L	+	++	++	Diffuse	6
R793M	+	++	++	Diffuse	6
Q930R	+	++	++	Diffuse	6
S973N	+	++	++	Diffuse	6
R1067Q	+	++	++	aggregate	4
S1096C	+	++	++	Diffuse	6
Q1111H	+	++	++	Diffuse	6
I1122V	+	++	++	Diffuse	6
A1151T	+	++	++	Diffuse	6
I1192V	+	++	++	Diffuse	6
S1228T	+	++	++	Diffuse	6
I1371V	+	++	++	Diffuse	6
R1441C	+	+	+	aggregate	2
R1441G	+	-	-	aggregate	2
R1441H	+	+	+	aggregate	2
A1442P	+	+	+	aggregate	2
R1514Q	+	++	++	Diffuse	6
V1613A	+	++	++	Diffuse	6
R1628P	+	++	++	Diffuse	6
Y1699C	+	-	-	aggregate	2
R1728H	++	++	++	Diffuse	1
R1728L	+	++	++	Diffuse	6
L1795F	+	+	-	aggregate	2
M1869T	+	++	++	Diffuse	6
E1874Stp	-	-	-	Diffuse	5
R1941H	+	++	++	Diffuse	6
Y2006H	+	++	++	Diffuse	6
I2012T	+	++	++	Diffuse	6
G2019S	+++	++	++	Diffuse	1
I2020T	+	-	-	aggregate	2
T2031S	++++	++	++	Diffuse	1
T2141M	+	++	++	Diffuse	6
R2143H	+	++	++	Diffuse	6
T2356I	+	++	++	Diffuse	6
G2385R	+	+	+	Diffuse	3
L2466H	+	++	++	Diffuse	6
910/935	+	-	-	aggregate	

Received 31 March 2010/16 July 2010; accepted 19 July 2010
Published as BJ Immediate Publication 19 July 2010, doi:10.1042/BJ20100483